The Relation of Glucose Metabolism to Left Ventricular Mass and Function and Sympathetic Nervous System Activity in Obese Subjects With Metabolic Syndrome

Nora E. Straznicky, Mariee T. Grima, Carolina I. Sari, Sofie Karapanagiotidis, Chiew Wong, Nina Eikelis, Katrina L. Richards, Geraldine Lee, Paul J. Nestel, John B. Dixon, Gavin W. Lambert, Markus P. Schlaich, and Elisabeth A. Lambert

Laboratories of Human Neurotransmitters (N.E.S., M.T.G., C.I.S., K.L.R., J.B.D., G.W.L., E.A.L.), Alfred Baker Medical Unit (S.K., C.W., G.L.), Neurovascular Hypertension and Kidney Disease (N.E., M.P.S.), and Cardiovascular Nutrition (P.J.N.), Baker IDI Heart and Diabetes Institute, Melbourne, Victoria 8008, Australia; and Faculty of Medicine, Nursing and Health Sciences (G.W.L., M.P.S.) and the Departments of Physiology (E.A.L.) and General Practice (J.B.D.), Monash University, Clayton 3800, and the Departments of Physiology (E.A.L.), Parkville 3010, and Cardiology (C.W.), Western Hospital, Footscray 3011, University of Melbourne, Melbourne, Victoria, Australia

Context: Altered cardiac structure and function have been reported in prediabetic and diabetic populations; however, the contribution of the sympathetic nervous system (SNS) to these changes has yet to be delineated.

Objective: Our objective was to examine interrelationships between glucose metabolism, left ventricular mass and function, and SNS activity in obese metabolic syndrome subjects.

Participants and Methods: Unmedicated impaired glucose tolerant (IGT) (n = 31) or treatment-naive type 2 diabetic (T2D) (n = 25) subjects, matched for age (mean 58 ± 1 years), gender, body mass index (32.2 ± 0.5 kg/m^2), and blood pressure, participated. They underwent echocardiography and assessments of whole-body norepinephrine kinetics, muscle sympathetic nerve activity, and insulin sensitivity by euglycemic clamp (M value).

Results: T2D subjects had higher left ventricular mass index (LVMI) (93.6 ± 3.5 vs 77.2 ± 3.4 g/m^2, $P = .002$) and Doppler-derived isovolumetric relaxation and deceleration times (both $P < .05$) and lower early/late transmitral inflow velocities (E/A) ($P = .02$) compared with IGT. Total muscle sympathetic nerve activity and arterial norepinephrine concentration were higher in the T2D group (by 18% and 32%, respectively, both $P \leq .05$), whereas plasma norepinephrine clearance was reduced (1.94 ± 0.11 vs 2.26 ± 0.10 L/min, $P = .02$). M value correlated inversely with left ventricular septal thickness ($r = -0.46$, $P = .007$). Whole-body noradrenaline spillover rate correlated with LVMI in the T2D subgroup ($r = 0.47$, $P = .03$). In the pooled cohort, LVMI was independently predicted by pulse pressure ($r = 0.38$, $P = .004$) and E/A ratio by 2-hour glucose ($r = -0.38$, $P = .005$).

Conclusions: Transition from IGT to T2D is associated with cardiac enlargement and diastolic dysfunction, which relate to metabolic, hemodynamic, and SNS alterations. **(*J Clin Endocrinol Metab* 98: E227–E237, 2013)**

Abbreviations: A, Late diastolic mitral inflow velocity; AUC, area under the curve; BMI, body mass index; BP, blood pressure; DHPG, 3,4-dihydroxyphenylglycol; E, early diastolic mitral inflow velocity; e', early diastolic tissue Doppler velocity; HOMA, homeostasis model assessment; HOMA-IR, HOMA for insulin resistance; hs-CRP, high-sensitivity C-reactive protein; IGT, impaired glucose tolerance; LDL, low-density lipoprotein; LV, left ventricular; LVMI, LV mass index; M, steady-state glucose utilization during euglycemic clamp, adjusted for fat-free mass; M/I, steady-state glucose utilization during euglycemic clamp, adjusted for fat-free mass and steady-state plasma insulin concentration; MSNA, muscle sympathetic nerve activity; NEFA, nonesterified fatty acid; NET, norepinephrine transporter; OGTT, oral glucose tolerance test; PRA, plasma renin activity; SNS, sympathetic nervous system; T2D, type 2 diabetes.

ISSN Print 0021-972X ISSN Online 1945-7197
Printed in U.S.A.

doi: 10.1210/jc.2012-3277 Received September 4, 2012. Accepted November 12, 2012.
First Published Online December 27, 2012

Type 2 diabetes (T2D) is an ongoing epidemic of growing dimensions in both Western and developing countries that currently affects 285 million adults (1). Overnutrition, sedentary lifestyle, and population aging as a consequence of socioeconomic development and urbanization, have fueled the rise in obesity, metabolic syndrome, and T2D prevalence (2). Cardiovascular diseases collectively represent the principal causes of death, disability, and excess healthcare costs associated with diabetes (3, 4). Individuals with T2D develop cardiovascular disease earlier in life, in more severe forms, and with a worse clinical prognosis than their nondiabetic counterparts (5, 6). Moreover, subclinical myocardial disease may be present even in the absence of ischemia and hypertension (7). Many interacting factors, comprising metabolic, hemodynamic, and autonomic derangements that promote structural myocardial changes, may be relevant to the association between abnormal glucose metabolism and cardiovascular morbidity and mortality (7–9).

Echocardiographic studies demonstrate that transition along the diabetic continuum is characterized by increased left ventricular (LV) mass and progressive impairment of LV diastolic function (10–12). Diabetic cardiomyopathy and heart failure are important clinical consequences, which may affect up to 26% of diabetic patients with LV dysfunction (13). The metabolic triumvirate of hyperglycemia, hyperinsulinemia, and hyperlipidemia have been identified as putative mediators of altered cardiac structure and function in diabetes, albeit coexistent hypertension exacerbates these pathophysiological processes (7, 10–12, 14). Glucose, insulin, and nonesterified fatty acids (NEFAs) are potent stimulants of the sympathetic nervous system (SNS) (15, 16), and reciprocally, sympathetic activation promotes insulin resistance (17) and lipolysis, hence perpetuating a vicious cycle. Elevated postganglionic muscle sympathetic nerve activity (MSNA) and arterial norepinephrine levels have been previously reported in T2D subjects compared with matched nondiabetic controls (9, 18). However, the relation of sympathetic activity and norepinephrine disposition to echocardiographic parameters is yet to be delineated in this clinical setting.

Anan et al (19) showed that within a cohort of T2D subjects, those with increased visceral fat accumulation had higher fasting insulin, greater impairment in LV diastolic function, and reduced myocardial uptake of [^{123}I]metaiodobenzylguanidine, a tracer taken up by sympathetic nerves via the norepinephrine transporter (NET). These findings concur with studies in rodent models of T2D in which sustained hyperglycemia is associated with elevated myocardial norepinephrine content, reduced cardiac [^{123}I]metaiodobenzylguanidine uptake, and decreased NET expression (20, 21). Increases in sympathetic tone could contribute to cardiac damage and dysfunction via effects on myocardial vascularity, endothelial function, apoptosis, angiotensin II signaling, reactive oxygen species production, and LV remodeling/hypertrophy (22, 23). In the present study, we sought to compare norepinephrine kinetics, MSNA, LV morphology, and function in age-, gender-, body mass index (BMI)-, and blood pressure (BP)-matched metabolic syndrome subjects, subclassified as having either impaired glucose tolerance (IGT) or treatment-naive T2D. A secondary aim was to examine metabolic, anthropometric, cardiovascular, and sympathetic correlates of LV mass and diastolic function to better understand the nature of pathogenic links.

Subjects and Methods

Subjects

Unmedicated, nonsmoking men (n = 27) and postmenopausal women (n = 29), mean age 58 ± 1 years and BMI 32.2 ± 0.5 kg/m^2, who fulfilled metabolic syndrome diagnostic criteria, having ≥3 abnormal findings as per the harmonized definition, participated (24). They were classified as IGT (fasting plasma glucose <7.0 mmol/L and 2-hour plasma glucose >7.8 and <11.1 mmol/L) or T2D (fasting plasma glucose ≥7.0 mmol/L or 2-hour glucose ≥11.1 mmol/L) after an oral glucose tolerance test (OGTT) (25). All consecutive T2D subjects participating in two clinical trials (NCT00408850 and NCT00163943) were included and matched by gender, age, BMI, and BP with IGT subjects from the same trials. Exclusion criteria included secondary hypertension, heart failure, prior history of autonomic neuropathy, cardiovascular, cerebrovascular, renal, liver, or thyroid disease, and treatment with medications that may influence study parameters (eg, hormone replacement therapy, antidepressants, cholesterol-lowering agents, antihypertensives, and oral hypoglycemic drugs). Supine BP was recorded by Dinamap monitor (model 1846SX; Critikon Inc., Tampa, FL) as the average of 5 readings after 5 minutes of rest. The study was approved by the Alfred Hospital Ethics Committee. All participants provided written informed consent.

Clinical investigations

Subjects attended at 8:00 AM on two mornings within a 7-day period, having fasted for 12 hours and abstained from caffeine and alcohol for 18 and 36 hours, respectively. They were instructed not to exercise on the day prior to investigations to eliminate acute effects of exercise. Anthropometric measurements comprised body weight, BMI, waist circumference, and waist to hip ratio. Body composition was measured by dual-energy x-ray absorptiometry (GE-LUNAR Prodigy Advance PA+130510; GE Medical Systems, Lunar, Madison, WI) scans. Experiments were conducted in a quiet room (temperature 22°C) with subjects lying in a supine position.

Echocardiography and Doppler imaging

Echocardiography was performed in the left decubitus position using a Vivid 7 ultrasound machine (GE Vingmed; GE

Healthcare) with an M4S 1.5- to 4.0-MHz matrix array probe, according to the guidelines of the American Society of Echocardiography (26, 27). LV wall thicknesses were measured from the 2-dimensional targeted M-mode echocardiographic tracings in the parasternal long axis view at the level of the mitral leaflet tips. LV mass was determined by the Devereux formula indexed to body surface area (LV mass index [LVMI]) (28). LV end-diastolic diameter and end-systolic volumes and LV ejection fraction were computed from 2- and 4-chamber views, using the modified Simpson's biplane method. Cardiac output was obtained from the LV outflow tract cross-sectional diameter and the velocity time integral measurements. Transmitral peaks of early (E) and late (A) diastolic mitral inflow velocities and E-wave deceleration time were recorded at the tips of the mitral valve leaflets. Peak tissue velocities were derived by tissue Doppler analysis at the septal and lateral margin of the mitral annulus for early diastolic tissue Doppler velocity (e′). Each representative value was obtained from the average of 3 measurements. All examinations were performed by an experienced research cardiac technologist (S.K.) and reported by a cardiologist (C.W.) who specialized in echocardiography, blinded to the metabolic status of participants.

SNS activity

Whole-body SNS activity was assessed using the radioisotope dilution method (29). This technique involves the iv infusion of [^{3}H]norepinephrine and measurement of norepinephrine specific activity and endogenous norepinephrine in arterial blood (sampled from the brachial artery) under steady-state conditions. The method provides a simultaneous estimate of the rate at which norepinephrine released from sympathetic nerve endings enters the plasma compartment (norepinephrine spillover) and norepinephrine plasma clearance. After a priming bolus of 1.94 μCi of 1-[ring-2,5,6-^{3}H]norepinephrine (PerkinElmer, Waltham, Massachusetts; specific activity, 10–30 μCi/mmol), an infusion was commenced at 0.094 $\mu Ci \cdot m^2 \cdot min^{-1}$. Plasma norepinephrine clearance and spillover rates were calculated as follows: norepinephrine clearance (liters per minute) = [^{3}H]norepinephrine infusion rate (disintegrations per minute per minute)/([^{3}H]norepinephrine plasma concentration [disintegrations per minute per milliliter] $\times$ 1000); norepinephrine spillover (nanograms per minute) = (plasma norepinephrine [picograms per milliliter] $\times$ clearance [milliliters per minute])/1000.

The rate of neuronal uptake of norepinephrine was estimated by measurement of its primary intraneuronal metabolite, 3,4-dihydroxyphenylglycol (DHPG). Steady-state [^{3}H]DHPG to [^{3}H]norepinephrine ratios were calculated as an index of NET function (29, 30).

Multiunit MSNA activity was measured by the technique of microneurography using a tungsten microelectrode inserted into a muscle nerve fascicle of the right peroneal nerve at the fibular head. Once an acceptable nerve-recording site was obtained via visual and acoustic identification of spontaneous sympathetic bursts, resting measurements were recorded over 15 minutes (18, 31). MSNA was manually analyzed and expressed as burst frequency (bursts per minute) and burst incidence (bursts per 100 heartbeats). Burst strength was quantified by defining the amplitude of the largest burst during the analyzed period as 100 and all other bursts as a percentage of the largest one, expressed as median burst amplitude. Total MSNA was calculated by multiplying median burst amplitude by burst frequency or burst incidence (units per minute and units per 100 heartbeats, respectively). Spontaneous cardiac baroreflex sensitivity was estimated by the sequence method of Parati as previously reported (18, 31).

Resting calf arterial blood flow was measured simultaneously in the left leg by venous occlusion plethysmography (D. E. Hokansen, Bellevue, Washington), based on the average of 12 consecutive measurements (31). Calf vascular resistance was calculated from Dinamap mean arterial pressure divided by mean calf blood flow.

Metabolic measurements

A 75-g OGTT (Glucaid; Fronine Pty Ltd, Taren Point, Australia) was performed on the same day as SNS tests with plasma glucose and insulin determination every 30 minutes. Fasting venous blood was obtained for measurement of lipid profile, NEFA, liver enzymes, uric acid, high-sensitivity C-reactive protein (hs-CRP) and plasma renin activity (PRA). Pancreatic β-cell function was evaluated by homeostasis model assessment (HOMA)-β and from area under the curve (AUC) for plasma concentration vs time of insulin to glucose between time 0 and 30 minutes during OGTT (32). Insulin resistance was assessed by HOMA for insulin resistance (HOMA-IR) and in a subset of 33 subjects (NCT00408850) by euglycemic-hyperinsulinemic clamp (32, 33). The clamp was initiated by an iv bolus injection of insulin (9 mU/kg; Actrapid 100 IU/ml; Novo Nordisk, Gentofte, Denmark), followed by a constant infusion rate of 40 $mU \cdot m^2 \cdot min^{-1}$ (18). Blood glucose was clamped at 5.0 mmol/L by the variable infusion of 25% glucose (Baxter, Toongabbie, Australia). The mean glucose infusion rate for the period 90 to 120 minutes was used to calculate whole-body glucose uptake, adjusted by fat-free mass (M) and steady-state plasma insulin concentration (M/I). Subjects provided a 24-hour urine specimen to quantify sodium, creatinine, and albumin excretion.

Laboratory analyses

Plasma glucose and lipid profile were quantified by automated enzymatic methods (Architect C18000 analyzer; Abbott Laboratories, Abbott Park, Illinois), hs-CRP by immunoturbidimetric assay, insulin and PRA by RIA (Linco Research, Inc, St Charles, Missouri; REN-CT2, Cis Bio International, Gif-sur-Yvette, France), and C-peptide by chemiluminescent immunoassay (ADVIA Centaur; Siemens Healthcare Diagnostics, Tarrytown, New York). Plasma norepinephrine and DHPG were determined by HPLC with electrochemical detection after extraction by alumina adsorption. [^{3}H]Norepinephrine and [^{3}H]DHPG in the effluent were assayed by liquid scintillation chromatography and the concentrations corrected for loss during extraction using recovery of internal standard. Intra-assay coefficients of variation in our laboratory are 1.3% for norepinephrine and 2.3% for [^{3}H]norepinephrine; interassay coefficients of variation are 3.8% and 4.5%, respectively. Corresponding values for DHPG and [^{3}H]DHPG are 2.0%, 6%, 8%, and 14%.

Statistical analyses

Normally distributed data are presented as mean ± SEM (95% confidence interval) and nonparametric data as median (interquartile range). Statistical analysis was performed using SigmaStat version 3.5 (Systat Software Inc, Point Richmond, California). The distribution of variables was examined by the

Table 1. Demographic and Clinical Variables of Study Participants

	IGT (n = 31)		T2D (n = 25)		
	Value[a]	95% CI	Value[a]	95% CI	*P* Value
Age, y	58 ± 1	56–59	59 ± 1	58–61	.14
Gender (male/female)	15/16		12/13		.88
Family history of T2D, n	14		9		.60
Hypertension,[b] n	20		20		.33
Anthropometrics					
Body weight, kg	94.4 ± 2.5	89.3–99.4	94.3 ± 3.6	86.9–101.7	.99
BMI, kg/m^2	32.0 ± 0.4	31.1–32.9	32.5 ± 1.0	30.5–34.5	.80
Waist circumference, cm	104.4 ± 1.6	101.1–107.7	106.8 ± 2.7	101.3–112.3	.42
Waist to hip ratio	0.91 ± 0.01	0.88–0.94	0.93 ± 0.02	0.89–0.96	.37
Total body fat, kg	37.4 ± 1.2	35.0–39.8	37.3 ± 2.0	33.1–41.5	.97
Trunk fat, kg	21.5 ± 0.6	20.3–22.8	21.5 ± 1.1	19.3–23.7	.99
Glucose metabolism					
Fasting glucose, mmol/L	5.8 ± 0.1	5.6–5.9	6.5 ± 0.2	6.1–6.9	<.001
2-h glucose, mmol/L	9.6 ± 0.1	9.3–9.9	13.9 ± 0.4	13.1–14.6	<.001
Glucose AUC_{0-120}, mmol/L/min	1188 ± 16	1156–1221	1462 ± 39	1381–1543	<.001
Fasting insulin, mU/L	19.9 ± 1.1	17.6–22.1	17.5 ± 1.1	15.3–19.7	.14
Insulin AUC_{0-120}, mU/L/min	12 118 ± 564	10 967–13 269	8504 ± 808	6837–10 171	<.001
Fasting C-peptide, pmol/L	830 ± 37	754–905	926 ± 73	775–1078	.21
HOMA-IR	5.09 ± 0.29	4.51–5.67	5.03 ± 0.33	4.34–5.71	.88
HOMA-β	183 ± 12	158–207	130 ± 13	104–156	<.001
Insulin AUC_{0-30}/glucose AUC_{0-30}	7.6 ± 0.4	6.9–8.4	5.1 ± 0.7	3.7–6.4	<.001
M, mg · kg FFM · min^{-1}[c]	10.2 ± 0.6	8.8–11.5	8.7 ± 0.8	6.8–10.5	.15
M/I, mg · kg FFM · min^{-1} · mU/L × 100[c]	9.2 ± 0.8	7.7–10.8	7.9 ± 0.8	6.2–9.6	.24
Lipids					
Total cholesterol, mmol/L	5.5 ± 0.2	5.2–5.9	5.4 ± 0.2	5.0–5.8	.64
LDL-cholesterol, mmol/L	3.6 ± 0.2	3.3–3.9	3.5 ± 0.2	3.1–3.8	.65
HDL-cholesterol, mmol/L	1.22 ± 0.04	1.13–1.31	1.20 ± 0.06	1.09–1.32	.79
Triglycerides, mmol/L	1.6 ± 0.1	1.4–1.8	1.6 ± 0.1	1.3–1.8	.92
NEFA, mEq/L	0.53 ± 0.03	0.47–0.59	0.57 ± 0.03	0.51–0.63	.33
Biochemistry					
Leptin, ng/mL	17.2 ± 1.9	13.3–21.1	17.9 ± 2.3	13.1–22.6	.82
hs-CRP, mg/L	2.8 ± 0.3	2.1–3.5	3.2 ± 0.5	2.2–4.2	.71
Uric acid, mmol/L	0.35 ± 0.01	0.33–0.38	0.33 ± 0.01	0.31–0.36	.33
γ-Glutamyl transferase, U/L	26 (21–33)		27 (22–43)		.23
Alanine aminotransferase, U/L	27 (19–39)		25 (20–31)		.27
Creatinine clearance, ml/min	130 ± 6	118–143	132 ± 8	117–148	.84
PRA, ng · ml · h^{-1}	0.70 ± 0.09	0.51–0.89	0.62 ± 0.07	0.49–0.75	.49
Urinary sodium, mmol/d	126 ± 9	108–145	163 ± 16	130–195	.08
Urinary albumin, mg/d[d]	19 ± 3	13–24	17 ± 2	13–21	.56

Abbreviations: CI, confidence interval; FFM, fat-free mass; M, steady-state glucose utilization during euglycemic clamp, adjusted for fat-free mass; M/I, steady-state glucose utilization during euglycemic clamp, adjusted for fat-free mass and steady-state plasma insulin concentration.

[a] Values are mean ± SEM or median (interquartile range) unless otherwise indicated.

[b] Hypertension defined as BP ≥130/85 mm Hg.

[c] Clamps were performed on 20 IGT and 13 T2D subjects.

[d] Albuminuria was detected in 14 IGT and 11 T2D subjects.

Kolmogorov-Smirnov test, and nonparametric data were log-transformed. Between-group differences were assessed by unpaired *t* test, Mann-Whitney *U* test and χ^2 test for proportions. The trapezoidal rule was used to calculate plasma glucose and insulin AUC during OGTT. T2D subjects were subclassified as insulin hypersecretors ($AUC_{0-120} > 8000$ mU/L/min) or hyposecretors ($AUC_{0-120} \leq 8000$ mU/L/min). Associations between parameters were assessed using linear regression analysis (Pearson's and Spearman's rank correlations). Forward stepwise regression analyses adjusted for age, gender, body weight, and BP were carried out with those univariate correlations where $P < .05$. A two-tailed *P* value <.05 was regarded as statistically significant.

Results

Subject characteristics

Demographic and clinical variables of participants are presented in Table 1. The two groups were matched for age, gender, body weight and composition, lipid profile, family history of diabetes, and proportion of hypertensive subjects, albeit pulse pressure was significantly higher in the T2D group (Table 2). Consistent with group allocation, diabetic subjects had higher fasting and 2-hour glucose and reduced pancreatic

Table 2. Cardiovascular and Echocardiographic Characteristics of Study Participants

	IGT (n = 31)		T2D (n = 25)		
	Value[a]	95% CI	Value[a]	95% CI	*P* Value
Clinic BP					
Systolic, mm Hg	133 ± 3	126–140	141 ± 3	135–147	.08
Diastolic, mm Hg	77 ± 2	73–80	76 ± 2	73–80	.78
Pulse pressure, mm Hg	56 ± 2	52–61	65 ± 2	60–70	.01
Heart rate, beats/min	63 ± 1	61–66	60 ± 1	57–63	.11
Cardiovascular					
CBF, ml · 100 g^{-1} · min^{-1}	2.13 ± 0.15	1.82–2.43	2.06 ± 0.19	1.68–2.45	.79
CVR, ml · 100 g^{-1} · min^{-1} · mm Hg	50 (38–68)		58 (43–75)		.59
Cardiac BRS, ms/mm Hg	12.3 (8.9–17.0)		13.3 (8.6–17.3)		.87
Echocardiography					
LVMI, g/m^2	77.2 ± 3.4	70.3–84.1	93.6 ± 3.5	86.3–101.0	.002
Septal wall thickness, mm	10.0 (9.3–11.0)		11.0 (10.3–12.0)		.024
Posterior wall thickness, mm	9.0 (8.0–10.0)		10.0 (8.3–11.0)		.036
LV end diastolic diameter, mm	47.6 ± 1.0	45.4–49.7	48.6 ± 0.9	46.8–50.4	.47
LV end systolic diameter, mm	29.7 ± 0.9	28.9–31.4	28.6 ± 1.1	26.3–30.9	.43
Fractional shortening, %	37.7 ± 1.2	35.2–40.1	42.2 ± 2.1	37.9–46.5	.048
LV ejection fraction, %	65.6 ± 1.2	62.6–67.5	66.3 ± 1.4	63.2–69.3	.75
Left atrial diameter, mm	37.0 (34.0–38.8)		40.0 (37.0–42.0)		.030
Left atrial volume index, ml/m^2	28.0 ± 1.2	25.0–30.0	29.4 ± 1.4	26.6–32.3	.47
Aortic root diameter, mm	32.0 (31.0–35.8)		35.0 (32.0–38.0)		.034
Cardiac output, L/min	4.8 (4.3–5.2)		5.1 (4.4–5.8)		.38
Doppler derived diastolic function					
E, m/s	0.70 (0.60–0.90)		0.70 (0.60–0.70)		.13
A, m/s	0.70 (0.60–0.80)		0.80 (0.70–0.80)		.032
E/A ratio	1.00 (0.73–1.20)		0.80 (0.70–1.00)		.022
Isovolumetric relaxation time, ms	106 ± 4	98–113	119 ± 6	108–131	.036
E wave deceleration time, ms	192 (179–213)		229 (190–248)		.026
Septal e′, cm/s	7.8 ± 0.3	7.3–8.3	7.1 ± 0.3	6.5–7.8	.09
Lateral e′, cm/s	10.0 (9.0–11.0)		10.0 (9.0–10.0)		.68
Mean E/e′ (septal and lateral)	8.6 ± 0.3	8.0–9.3	8.5 ± 0.4	7.8–9.2	.78

Abbreviations: BRS, baroreflex sensitivity; CBF, calf blood flow; CI, confidence interval; CVR, calf vascular resistance.

[a] Values are the mean ± SEM or median (interquartile range).

β-cell function, evidenced by lower HOMA-β, insulin AUC_{0-30} to glucose AUC_{0-30} ratio, and overall insulin response during OGTT vs the IGT group. Insulin sensitivity quantified as HOMA-IR, M, and M/I values did not differ significantly between groups. Within the T2D group, 10 subjects were insulin hypersecretors and 15 were hyposecretors (insulin AUC_{0-120} 12 377 ± 1160 and 5921 ± 311 mU/L/min, respectively).

Echocardiographic parameters

Echocardiographic evaluation (Table 2) showed that T2D subjects had higher LVMI including septal and posterior wall thicknesses. Based on M-mode linear cutpoints, 4 T2D and 1 IGT subject was classified as having LV hypertrophy (26). Left atrial and aortic root diameters were also significantly greater in the T2D group. Doppler measurements of mitral inflow indicated higher late diastolic filling (A-wave) velocity, lower E/A ratio, and increased deceleration and isovolumetric relaxation times in the T2D compared with IGT group (all $P < .05$). Tissue Doppler recording of early diastolic velocity at the septal side of the mitral annulus tended to be lower in the T2D group ($P = .09$), whereas E/e′ ratios did not differ. Echocardiographic parameters did not differ between hyperinsulinemic and hypoinsulinemic T2D subgroups.

SNS activity

T2D subjects had higher arterial norepinephrine concentration (by 32%), reduced neuronal norepinephrine reuptake based on the [^{3}H]DHPG to [^{3}H]norepinephrine ratio (by 53%), and reduced plasma norepinephrine clearance (by 16%) (all $P \leq 0.05$, Figure 1). Norepinephrine spillover rate did not differ between groups. Successful microneurographic recordings were available for 29 IGT and 22 T2D subjects. Analyses demonstrated higher median burst amplitude in the T2D group (50 ± 2% vs 45 ± 2%, $P = .05$) and greater total MSNA (3715 ± 240 vs 3144 ± 171 U/100 heartbeats, $P = .05$) compared with the IGT group. Burst frequency (41 ± 2 vs 40 ± 1 bursts/min) and incidence (71 ± 4 vs 67 ± 3 bursts/100 heartbeats) were similar. Spontaneous cardiac baroreflex sensitivity

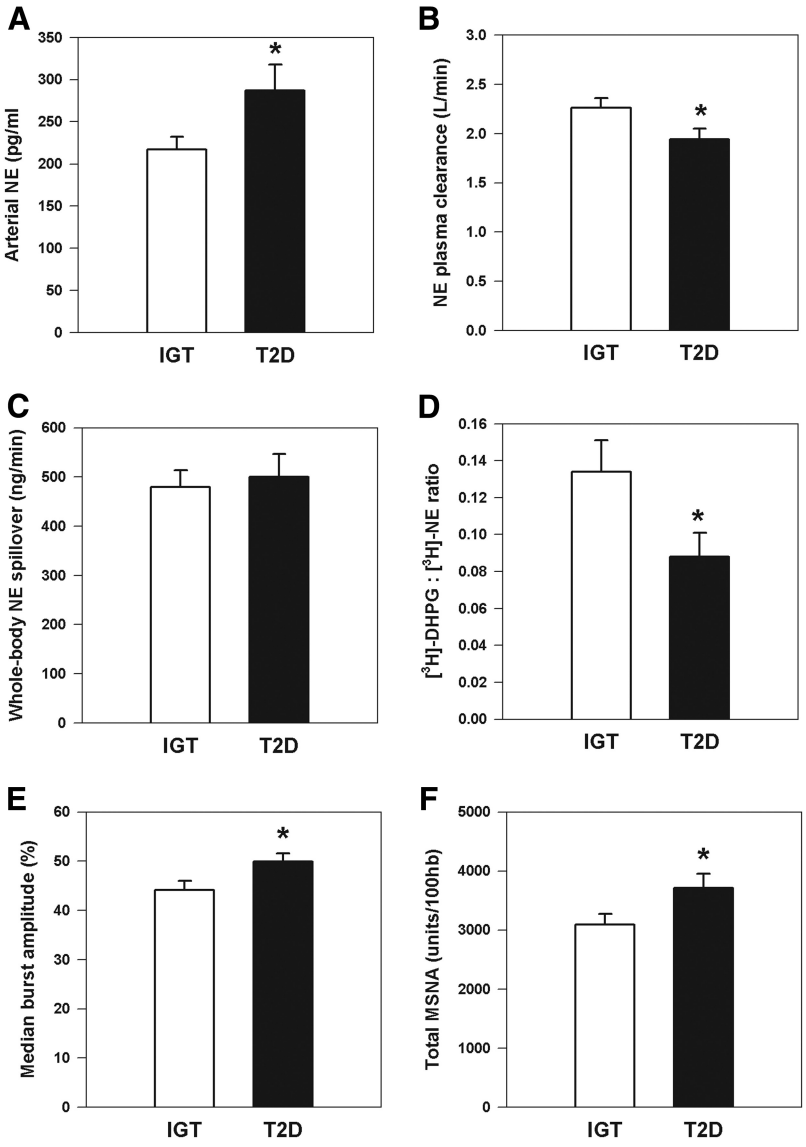

Figure 1. SNS parameters in IGT and T2D subjects. A, Arterial norepinephrine (NE) concentration. B, Norepinephrine plasma clearance. C, Whole-body norepinephrine spillover. D, Neuronal uptake of norepinephrine estimated as the ratio of plasma tritiated DHPG to tritiated norepinephrine concentration ([^{3}H]DHPG:[^{3}H]NE). E, MSNA median burst amplitude. F, Total MSNA expressed as units per 100 heartbeats. *$P \leq .05$ vs IGT.

and calf vascular resistance did not differ between groups (Table 2).

Correlation and regression analyses

Key metabolic correlates of LV mass and function are presented in Figure 2. LVMI correlated with clinic systolic pressure ($r = 0.42$, $P = .002$) and pulse pressure ($r = 0.38$, $P = .004$), waist to hip ratio ($r = 0.34$, $P = .01$), plasma leptin ($r = -0.42$, $P = .002$), γ-glutamyl transferase concentrations ($r = 0.36$, $P = .008$), gynoid fat mass ($r = -0.27$, $P = .05$), and clamp-derived M value ($r = -0.34$, $P = .05$). Sympathetic neural parameters did not correlate with LV structure overall; however, within the T2D subgroup, norepinephrine spillover was associated with LVMI ($r = 0.47$, $P = .026$).

Age, glucose tolerance, and fasting C-peptide levels were the strongest correlates of diastolic function. Two-hour glucose concentration was associated with E ($r = -0.28$, $P = .04$), A ($r = 0.31$, $P = .02$), E/A ratio ($r = -0.38$, $P = .005$), mitral deceleration time ($r = 0.32$, $P = .02$), and norepinephrine disposition (plasma clearance, $r = -0.34$, $P = .01$; [^{3}H]DHPG to [^{3}H]norepinephrine ratio, $r = -0.26$, $P = .05$) (Figure 3). In turn, [^{3}H]DHPG to [^{3}H]norepinephrine ratio was correlated with E ($r = 0.36$, $P = .009$), arterial norepinephrine concentration with A ($r = 0.29$, $P = .03$), and total MSNA burst incidence with A ($r = 0.28$, $P = .05$). Among the metabolic variables, both fasting C-peptide and NEFA concentrations were inversely related to E/A ratio ($r = -0.38$, $P = .005$; $r = -0.37$, $P = .006$, respectively). Total MSNA was associated with glucose AUC_{0-120} ($r = 0.30$, $P = .03$), triglycerides ($r = 0.44$, $P = .001$), NEFA ($r = 0.28$, $P = .05$), low-density lipoprotein (LDL)-cholesterol ($r = 0.33$, $P = .02$) and hs-CRP ($r = 0.27$, $P = .05$) concentrations. Norepinephrine spillover related to NEFA ($r = 0.27$, $P = .046$) and PRA ($r = 0.32$, $P = .02$).

In stepwise regression analyses (Table 3), pulse pressure and plasma leptin concentration (inverse) were the only independent predictors of LVMI, accounting for 28% of the variance. C-peptide levels and calf vascular resistance predicted LV septal thickness, whereas body weight, trunk fat mass, pulse pressure, and 2-hour glucose concentration predicted LV posterior thickness. Age and glucose tolerance were independent inverse predictors of diastolic function accounting for 18% to 30% of the variance. Paradoxically, total cholesterol and LDL-cholesterol were independent inverse predictors of E/A ratio and isovolumetric relaxation time, respectively.

Discussion

This study was performed to examine interrelationships among glucose tolerance status, SNS activity, and echocardiographic measures of LV structure and function within a cohort of obese, untreated metabolic syndrome subjects. Consistent with previous reports, our data demonstrate that transition from IGT to T2D is accompanied

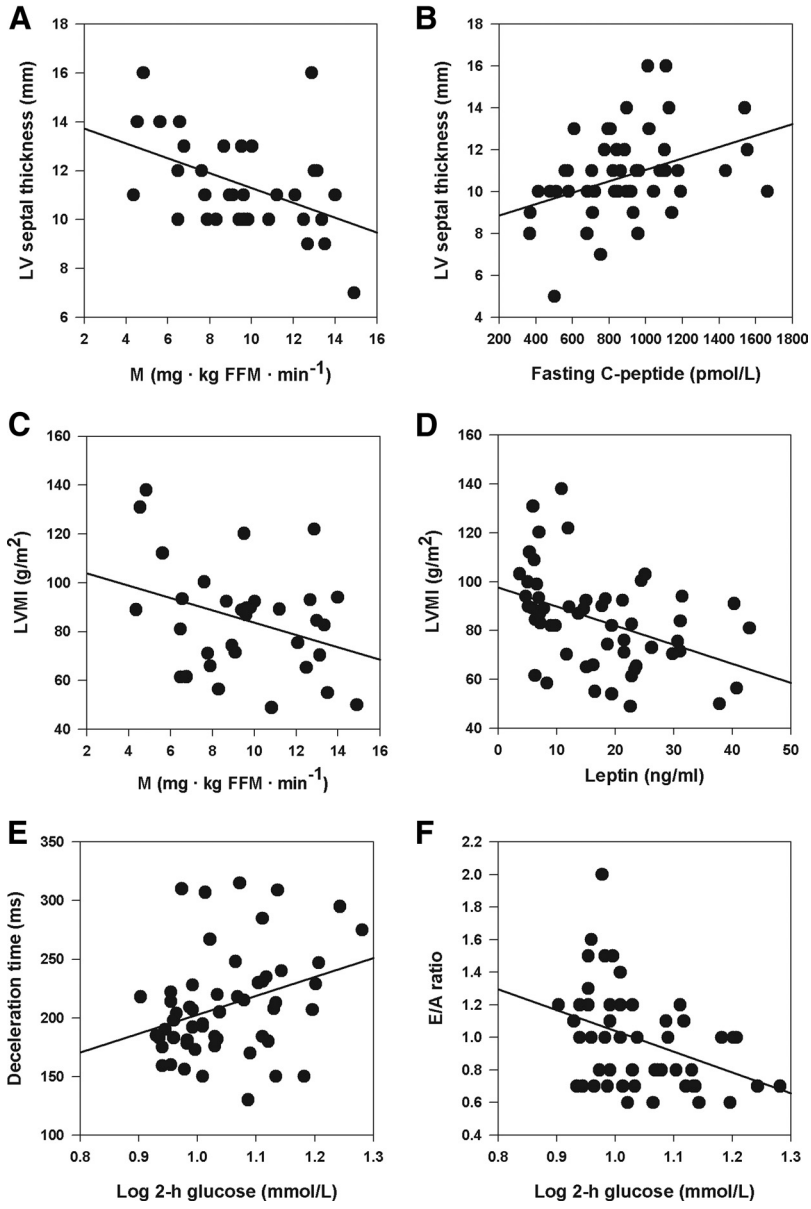

Figure 2. Metabolic correlates of LV mass and function in the pooled cohort. A, Steady-state glucose utilization during euglycemic-hyperinsulinemic clamp (M) versus LV septal thickness ($r = -0.46$, $P = .007$). B, Plasma fasting C-peptide vs LV septal thickness ($r = 0.38$, $P = .005$). C, M value vs LVMI ($r = -0.34$, $P = .05$). D, Fasting plasma leptin concentration vs LVMI ($r = -0.42$, $P = .002$). E, E-wave deceleration time vs 2-hour plasma glucose during OGTT ($r = 0.32$, $P = .02$). F, E/A ratio vs 2-hour plasma glucose during OGTT ($r = -0.38$, $P = .005$).

by cardiac enlargement and diastolic dysfunction, characterized by impaired LV relaxation, and reduced early and increased late diastolic Doppler flow velocities (10, 11). A novel, hitherto unreported finding is that echocardiographic changes are paralleled by alterations in norepinephrine disposition in T2D subjects. Reductions in both neuronal uptake (uptake 1) and plasma clearance, and concomitant elevation in arterial norepinephrine levels, were evident in the absence of increased norepinephrine spillover rate. Moreover, direct recordings of efferent postganglionic sympathetic nerve traffic directed at skeletal muscle vasculature showed increased burst amplitude and hence total MSNA in the T2D vs IGT group. Regression analyses indicated that hemodynamic factors (pulse pressure and calf vascular resistance), central adiposity (trunk fat mass), and fasting C-peptide concentration were independent positive predictors of LV mass. In turn, age and the degree of impairment of glucose metabolism were the strongest independent predictors of LV diastolic dysfunction.

Hyperglycemia, excess NEFA, and insulin resistance are recognized pathophysiological substrates of diabetic cardiomyopathy that engender adverse metabolic events and subsequent changes in cardiac structure and function (7, 34). Hyperinsulinemia can lead to increased myocardial mass through its growth-stimulating effects and via chronic activation of the SNS (14, 15). In addition, impairment in phosphatidylinositol 3-kinase-dependent signaling contributes to reciprocal relationships between endothelial dysfunction and insulin resistance (35). Our study demonstrated a significant inverse relationship between LV mass and insulin sensitivity, measured by the gold standard euglycemic-hyperinsulinemic clamp technique. In the pooled cohort, fasting C-peptide, a surrogate marker for insulin secretion, was independently associated with LV septal thickness. Diastolic abnormalities may occur as a consequence of either hypertrophy or hyperglycemia (7). Hyperglycemia mediates myocardial and arterial tissue injury through various pathways, including the formation of advanced glycation end products and reactive oxygen species, alterations in myocardial calcium handling, and posttranslational modification of the extracellular matrix, which promote impaired LV relaxation and increased ventricular stiffness (7, 34). Early alterations in cardiac function in relation to glucose tolerance status are highlighted by findings in hypertensive patients with normal glucose tolerance, showing that 1-hour oral postload plasma glucose level was associated with LV dysfunction (11). In our group of IGT and newly diagnosed T2D subjects, glucose metabolism was strongly and independently related to indices of LV diastolic function. Similarly, NEFA concentrations, which play a critical role in the development of insulin resistance, as well as directly affecting myocardial contractility (7), were inversely related to E/A ratio.

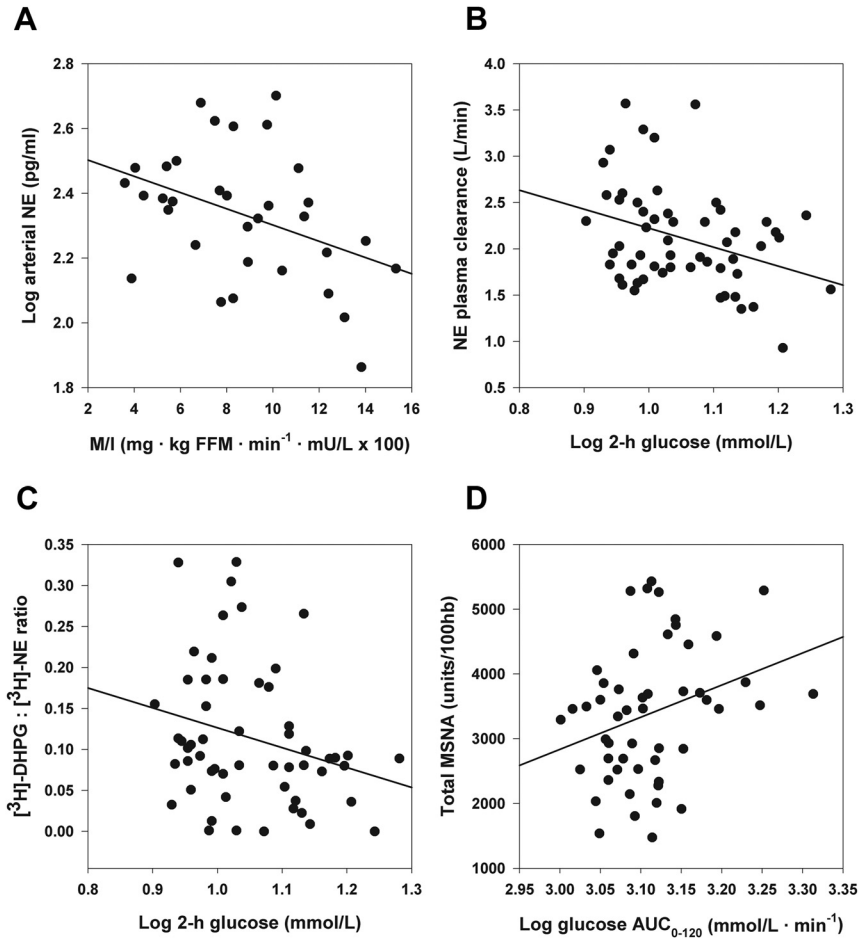

Figure 3. Relation of glucose metabolism to sympathetic neural parameters. A, Arterial norepinephrine (NE) concentration vs steady-state glucose utilization adjusted by steady-state plasma insulin concentration (M/I) ($r = -0.40$, $P = .02$). B, Norepinephrine plasma clearance vs 2-hour plasma glucose during OGTT ($r = -0.34$, $P = .01$). C, Neuronal norepinephrine reuptake, estimated as the ratio of [^{3}H]DHPG to [^{3}H]NE, vs 2-hour plasma glucose concentration ($r = -0.26$, $P = .05$). D, Total MSNA vs plasma glucose AUC during OGTT ($r = 0.30$, $P = .03$).

Prospective cohort studies suggest that autonomic dysfunction may be a mechanism associated with early glucose dysmetabolism and the development of diabetes (36, 37). The Atherosclerosis Risk in Communities Study showed that participants with higher baseline heart rate and reduced low frequency power of heart rate variability were at an increased risk of incident T2D after adjustment for confounders such as age, BMI, and physical activity (36). Vis-à-vis, there is ample evidence that diabetes leads to subsequent autonomic nervous system dysfunction, comprising elevated resting sympathetic neural tone and blunted sympathetic responsiveness (9, 18) and, in the longer term, to cardiac autonomic neuropathy and sympathetic dysinnervation (34). Our findings highlight that alterations in norepinephrine disposition are evident early in the genesis of diabetes, because our subjects were all newly diagnosed and treatment-naive. Arterial norepinephrine concentration is a function of two dynamic processes: norepinephrine release by sympathetic nerve endings and clearance from the synaptic cleft and central plasma compartment. It is estimated that 90% of released norepinephrine undergoes immediate neuronal reuptake via active transport processes involving NET, and thus only 10% spills over into the circulation (30). In our study, neuronal norepinephrine uptake was on average 53% lower, whereas plasma norepinephrine clearance was 16% lower in the T2D compared with IGT subjects, resulting in significantly higher arterial norepinephrine concentration. Both neuronal uptake and plasma clearance were inversely correlated with measures of glucose metabolism.

Animal studies provide temporal assessments of the effects of sustained hyperglycemia on cardiac SNS integrity. Using a high-fat diet-fed streptozotocin rat model, Thackeray et al (21) showed that 8 weeks of hyperglycemia was associated with elevated myocardial norepinephrine content, up to 25% reduction in [^{11}C]*meta*-hydroxyephedrine uptake, a 17% reduction in NET transporter expression, and no change in sympathetic nerve density . This study provides evidence that alterations in NET function and/or expression can precede sympathetic dysinnervation. A growing body of data suggests that insulin may be an important inhibitory regulator of NET function by acutely and chronically suppressing NET expression and surface availability (38, 39). Hyperglycemia may also have a deleterious effect on NET expression via enhanced polyol formation, because blockade of this pathway with aldose reductase inhibitor protects against the reduction in myocardial NET protein in streptozotocin-treated rats (40). Our group has previously reported reduced cardiac release of [^{3}H]DHPG in lean hypertensives vs healthy controls (41); thus, essential hypertension may also modulate NET. The liver and the kidneys contribute significantly to extraneuronal removal of circulating catecholamines, and factors such as transporter affinity and regional blood flow may influence plasma clearance of norepinephrine at these sites (30). It is anticipated that impaired neuronal reuptake and plasma clearance would have important cardiac and metabolic effects,

Table 3. Stepwise Regression Analyses of Echocardiographic Variables in the Pooled Cohort

Dependent Variables	Step	Independent Predictor Variables	R^2	Association	*P*
LVMI, g/m^2	1	Fasting plasma leptin, ng/mL	0.18	Inverse	.004
	2	Pulse pressure, mm Hg	0.28	Positive	.009
LV septal thickness, mm	1	C-peptide, pmol/L	0.16	Positive	.003
	2	Log calf vascular resistance, U	0.25	Positive	.019
LV posterior thickness, mm	1	Body weight, kg	0.38	Positive	<.001
	2	Trunk fat mass, kg	0.47	Positive	<.001
	3	Pulse pressure, mm Hg	0.56	Positive	.009
	4	Triglycerides, mmol/L	0.62	Inverse	.005
	5	Log 2-h plasma glucose, mmol/L	0.66	Positive	.022
Mitral E/A ratio	1	Age, y	0.22	Inverse	.002
	2	Log 2-h plasma glucose, mmol/L	0.30	Inverse	.025
E wave deceleration time, ms	1	Age, y	0.18	Positive	<.001
	2	Total cholesterol, mmol/L	0.32	Inverse	.002
Isovolumetric relaxation time, ms	1	LDL-cholesterol, mmo/L	0.15	Inverse	.005
	2	Log glucose AUC_{0-120}, mmol/L/min	0.25	Positive	.043

R^2 is the coefficient of determination for stepwise regression.

secondary to increased adrenergic stimulation. Indeed, in our study, arterial noradrenaline concentration was inversely correlated with glucose utilization, whereas total MSNA was associated with glucose AUC_{0-120} and hyperlipidemia. Although whole-body norepinephrine spillover rate correlated with LVMI in the T2D subgroup, sympathetic nervous activity was not an independent predictor of LV mass or diastolic function in the present study, suggesting that it may be an intermediary player in the pathogenesis of diabetic cardiomyopathy that promotes hemodynamic and metabolic perturbations. It merits emphasis that our subjects were in the early stages of diabetes, with only a small proportion having LV hypertrophy. With further disease progression and more advanced LV hypertrophy, interrelationships with sympathetic nervous activity may become more pronounced (23). Also, organ-specific measures of sympathetic activity, such as cardiac norepinephrine spillover, may provide a more sensitive assessment in relation to cardiac function than the more ubiquitous whole-body norepinephrine spillover used herein (23).

The present study has several limitations. First, we investigated only subjects with IGT and T2D and had no controls with normal glucose tolerance. Second, we did not measure hemoglobin A_{1c},and classification of subjects was based on a single OGTT. Third, our sample size was relatively small, and only a subset of subjects underwent clamp experiments. Fourth, our diabetic cohort was heterogeneous, comprising both insulin hypersecretors and hyposecretors, which represent distinct stages in the pathogenesis of T2D and warrant further separate investigation in larger studies. Finally, because this analysis was cross-sectional, no conclusions about causality can be drawn. In summary, our study findings extend previous echocardiographic observations that worsening glucose metabolism is associated with cardiac enlargement and LV diastolic dysfunction. We have for the first time demonstrated parallel increases in MSNA and alterations in norepinephrine disposition in T2D subjects, consistent with increased cardiometabolic risk. Future research needs to examine whether treatment strategies such as weight loss, exercise, and insulin-sensitizing drugs that target the metabolic triumvirate of hyperglycemia, hyperinsulinemia and hyperlipidemia restore sympathetic neural dysfunction and protect the myocardium from further damage.

Acknowledgments

We thank the study participants for their cooperation and effort and research nurses Donna Vizi and Jenny Starr (Alfred Baker Medical Unit, Baker IDI Heart and Diabetes Institute) for their excellent assistance.

Address all correspondence and requests for reprints to: Dr Nora E. Straznicky, Baker IDI Heart and Diabetes Institute, PO Box 6492, St. Kilda Road Central, Melbourne, Victoria 8008, A. E-mail: Nora.Straznicky@bakeridi.edu.au.

The study was funded by a Heart Foundation Grant-in-Aid (G11M5892) and a Diabetes Australia Millennium Grant to N.E.S. J.B.D., M.P.S., and G.W.L. are supported by NHMRC Fellowships. We also acknowledge the Victorian Government's Operational Infrastructure Support Program.

Disclosure Summary: N.E.S., M.T.G., C.I.S., S.K., C.W., N.E., K.L.R., G.L., and E.A.L. have nothing to declare. P.J.N. has consultative and advisory board associations with Merck Sharp & Dohme and Astra Zeneca. J.B.D. receives competitive research grant funding from Allergan Inc. He is a consultant for Allergan Inc., Bariatric Advantage, and Scientific Intake and is a member of the Optifast Medical Advisory Board for Nestle Health, Australia. He is on the speakers bureaus for Eli Lilly and iNova Pharmaceuticals, has developed educational material for Novartis and iNova Pharma-

ceuticals, and received travel assistance from GI Dynamics for an educational meeting. M.P.S. serves on scientific advisory boards for Abbott Pharmaceuticals, Novartis Pharmaceuticals, and Medtronic. G.W.L. has acted as a consultant for Medtronic and has received honoraria from Medtronic, Pfizer, and Wyeth Pharmaceuticals for presentations. These organizations played no role in the design, analysis, or interpretation of data described here or in the preparation, review, or approval of the manuscript.

References

1. **Shaw JE, Sicree RA, Zimmet PZ.** Global estimates of the prevalence of diabetes for 2010 and 2030. *Diabetes Res Clin Pract*. 2010;87:4–14.
2. **Chan JC, Malik V, Jia W, et al.** Diabetes in Asia. Epidemiology, risk factors, and pathophysiology. *JAMA*. 2009;301:2129–2140.
3. **Barr EL, Zimmet PZ, Welborn TA, et al.** Risk of cardiovascular and all-cause mortality in individuals with diabetes mellitus, impaired fasting glucose, and impaired glucose tolerance: The Australian Diabetes, Obesity, and Lifestyle Study (AusDiab). *Circulation*. 2007;116:151–157.
4. **Ariza MA, Vimalananda VG, Rosenzweig JL.** The economic consequences of diabetes and cardiovascular disease in the United States. *Rev Endocrinol Metab Disord*. 2010;11:1–10.
5. **Natali A, Vichi S, Landi P, Severi S, L'Abbate A, Ferrannini E.** Coronary atherosclerosis in type II diabetes: angiographic findings and clinical outcomes. *Diabetologia*. 2000;43:632–641.
6. **Bonow RO, Gheorghiade M.** The diabetes epidemic: A national and global crisis. *Am J Med*. 2004;116:2S–10S.
7. **Poornima IG, Parikh P, Shannon RP.** Diabetic cardiomyopathy. The search for a unifying hypothesis. *Circ Res*. 2006;98:596–605.
8. **Perciaccante A, Fiorentini A, Paris A, Serra P, Tubani L.** Circadian rhythm of the autonomic nervous system in insulin resistant subjects with normoglycemia, impaired fasting glycemia, impaired glucose tolerance, type 2 diabetes mellitus. *BMC Cardiovascular Disorders*. 2006;6:19.
9. **Huggett RJ, Scott EM, Gilbey SG, Stoker JB, Mackintosh AF, Mary DA.** Impact of type 2 diabetes on sympathetic neural mechanisms in hypertension. *Circulation*. 2003;108:3097–3101.
10. **Stahrenberg R, Edelmann F, Mende M, et al.** Association of glucose metabolism with diastolic function along the diabetic continuum. *Diabetologia*. 2010;53:1331–1340.
11. **Sciacqua A, Miceli S, Greco L, et al.** One-hour postload plasma glucose levels and diastolic function in hypertensive patients. *Diabetes Care*. 2011;34:2291–2296.
12. **Dinh W, Lankisch M, Nickl W, et al.** Insulin resistance and glycemic abnormalities are associated with deterioration of left ventricular diastolic function: a cross-sectional study. *Cardiovasc Diabetol*. 2010;9:63.
13. **Schindler DM, Kostis JB, Yusuf S, et al.** Diabetes mellitus, a predictor of morbidity and mortality in the studies of Left Ventricular Dysfunction (SOLVD) Trials and Registry. *Am J Cardiol*. 1996;77:1017–1020.
14. **Holmang A, Yoshida N, Jennische E, Waldenstrom A, Bjorntorp P.** The effects of hyperinsulinemia on myocardial mass, blood pressure regulation and central haemodynamics in rats. *Eur J Clin Invest*. 1996;26:973–978.
15. **Anderson EA, Hoffman RP, Balon TW, Sinkey CA, Mark AL.** Hyperinsulinemia produces both sympathetic neural activation and vasodilation in normal humans. *J Clin Invest*. 1991;87:2246–2252.
16. **Florian JP, Pawelczyk JA.** Non-esterified fatty acids increase arterial pressure via central sympathetic activity in humans. *Clin Sci*. 2010;118:61–69.
17. **Jamerson KA, Julius S, Gudbrandsson T, Andersson O, Brant DO.** Reflex sympathetic activation induces acute insulin resistance in human forearm. *Hypertension*. 1993;21:618–623.
18. **Straznicky NE, Grima MT, Sari CI, et al.** Neuroadrenergic dysfunction along the diabetic continuum: A comparative study in obese metabolic syndrome subjects. *Diabetes*. 2012;61:2506–2516.
19. **Anan F, Masaki T, Yonemochi H, et al.** Abdominal visceral fat accumulation is associated with the results of ^{123}I-metaiodobenzylguanidine myocardial scintigraphy in type 2 diabetes. *Eur J Nucl Med Mol Imaging*. 2007;34:1189–1197.
20. **Kiyono Y, Lida Y, Kawashima H, et al.** Norepinephrine transporter density as a causative factor in alterations in MIBG myocardial uptake in NIDDM model rats. *Eur J Nucl Med Mol Imaging*. 2002;29:999–1005.
21. **Thackeray JT, Radziuk J, Harper ME, et al.** Sympathetic nervous dysregulation in the absence of systolic left ventricular dysfunction in a rat model of insulin resistance and hyperglycemia. *Cardiovasc Diabetol*. 2011;10:75.
22. **Pop-Busui R, Kirkwood I, Schmid H, et al.** Sympathetic dysfunction in type 1 diabetes. Association with impaired myocardial blood flow reserve and diastolic dysfunction. *J Am Coll Cardiol*. 2004;44:2368–2374.
23. **Schlaich MP, Kaye DM, Lambert E, Sommerville M, Socratous F, Esler MD.** Relation between cardiac sympathetic activity and hypertensive left ventricular hypertrophy. *Circulation*. 2003;108:560–565.
24. **Alberti KG, Eckel RH, Grundy SM, et al.** Harmonizing the metabolic syndrome. A joint interim statement of the International Diabetes Federation Task Force on Epidemiology and Prevention; National Heart, Lung and Blood Institute; American Heart Association; World Heart Federation; International Atherosclerosis Society; and International Association for the Study of Obesity. *Circulation* 2009;120:1640–1645.
25. **World Health Organization.** *Definition and Diagnosis of Diabetes Mellitus and Intermediate Hyperglycaemia: Report of a WHO/IFD Consultation*. Geneva, Switzerland: World Health Organization; 2006.
26. **Lang RM, Bierig M, Devereux RB, et al.** Recommendations for chamber quantification: a report from the American Society of Echocardiography's Guidelines and Standards Committee and the Chamber Quantification Writing Group, developed in conjunction with the European Association of Echocardiography, a branch of the European Society of Cardiology. *J Am Soc Echocardiogr*. 2005;18:1440–1463.
27. **Nagueh SF, Appleton CP, Gillebert TC, et al.** Recommendations for the evaluation of left ventricular diastolic function by echocardiography. *J Am Soc Echocardiogr*. 2009;22:107–133.
28. **Devereux RB, Reichek N.** Echocardiographic determination of left ventricular mass in man. Anatomic validation of the method. *Circulation*. 1977;55:613–618.
29. **Eisenhofer G.** Sympathetic nerve function. Assessment by radioisotope dilution analysis. *Clin Auton Res*. 2005;15:264–283.
30. **Eisenhofer G, Goldstein DS, Kopin IJ.** Plasma dihydroxyphenylglycol for estimation of noradrenaline neuronal re-uptake in the sympathetic nervous system *in vivo*. *Clin Sci*. 1989;76:171–182.
31. **Straznicky NE, Lambert GW, Masuo K, et al.** Blunted sympathetic neural response to oral glucose in obese subjects with the insulin-resistant metabolic syndrome. *Am J Clin Nutr*. 2009;89:27–36.
32. **Matthews DR, Hosker JP, Rudenski AS, Naylor BA, Treacher DF, Turner RC.** Homeostasis model assessment: insulin resistance and β-cell function from fasting plasma glucose and insulin concentrations in man. *Diabetologia*. 1985;28:412–419.
33. **DeFronzo RA, Tobin JD, Andres R.** Glucose clamp technique: a method for quantifying insulin secretion and resistance. *Am J Physiol*. 1979;6:E214–E223.
34. **Voulgari C, Papadogiannis D, Tentolouris N.** Diabetic cardiomyopathy: from the pathophysiology of the cardiac myocytes to current

diagnosis and management strategies. *Vasc Health Risk Man*. 2010; 6:883–903.
35. **Muniyappa R, Quon MJ.** Insulin action and insulin resistance in vascular endothelium. *Curr Opin Clin Nutr Metab Care*. 2007;10: 523–530.
36. **Carnethon MR, Golden SH, Folsom AR, Haskell W, Liao D.** Prospective investigation of autonomic nervous system function and the development of type 2 diabetes. The Atherosclerosis Risk in Communities Study, 1987–1998. *Circulation*. 2003;107: 2190–2195.
37. **Carnethon MR, Prineas RJ, Temprosa M, Zhang ZM, Uwaifo G, Molitch ME.** The association among autonomic nervous system function, incident diabetes, and intervention arm in the Diabetes Prevention Program. *Diabetes Care*. 2006;29:914–919.
38. **Figlewicz DP, Szot P, Israel PA, Payne C, Dorsa DM.** Insulin reduces norepinephrine transporter mRNA in vivo in rat locus coeruleus. *Brain Res*. 1993;602:161–164.
39. **Robertson SD, Matthies HJ, Owens WA, et al.** Insulin reveals Akt signalling as a novel regulator of norepinephrine transporter trafficking and norepinephrine homeostasis. *J Neurosci*. 2010;30: 11305–11316.
40. **Kiyono Y, Kajiyama S, Fujiwara H, Kanegawa N, Saji H.** Influence of the polyol pathway on norepinephrine transporter reduction in diabetic cardiac sympathetic nerves: implications for heterogeneous accumulation of MIBG. *Eur J Nucl Med Mol Imaging*. 2005;32: 438–442.
41. **Rumantir MS, Kaye DM, Jennings GL, Vaz M, Hastings JA, Esler MD.** Phenotypic evidence of faulty neuronal norepinephrine reuptake in essential hypertension. *Hypertension*. 2000;36:824–829.